Recoil Polarization for Δ Excitation in Pion Electroproduction

J. J. Kelly,[1] R. E. Roché,[2] Z. Chai,[3] M. K. Jones,[4] O. Gayou,[3] A. J. Sarty,[5] S. Frullani,[6] K. Aniol,[7] E. J. Beise,[1]
F. Benmokhtar,[8] W. Bertozzi,[3] W. U. Boeglin,[9] T. Botto,[10] E. J. Brash,[11] H. Breuer,[1] E. Brown,[12] E. Burtin,[13]
J. R. Calarco,[14] C. Cavata,[13] C. C. Chang,[1] N. S. Chant,[1] J.-P. Chen,[4] M. Coman,[9] D. Crovelli,[8] R. De Leo,[6] S. Dieterich,[8]
S. Escoffier,[13] K. G. Fissum,[15] V. Garde,[16] F. Garibaldi,[6] S. Georgakopoulos,[10] S. Gilad,[3] R. Gilman,[8] C. Glashausser,[8]
J.-O. Hansen,[4] D. W. Higinbotham,[3] A. Hotta,[17] G. M. Huber,[11] H. Ibrahim,[18] M. Iodice,[6] C. W. de Jager,[4] X. Jiang,[8]
A. Klimenko,[18] A. Kozlov,[11] G. Kumbartzki,[8] M. Kuss,[4] L. Lagamba,[6] G. Laveissière,[16] J. J. LeRose,[4] R. A. Lindgren,[19]
N. Liyanage,[4] G. J. Lolos,[11] R. W. Lourie,[20] D. J. Margaziotis,[7] F. Marie,[13] P. Markowitz,[9] S. McAleer,[2] D. Meekins,[2]
R. Michaels,[4] B. D. Milbrath,[21] J. Mitchell,[4] J. Nappa,[8] D. Neyret,[13] C. F. Perdrisat,[22] M. Potokar,[23] V. A. Punjabi,[24]
T. Pussieux,[13] R. D. Ransome,[8] P. G. Roos,[1] M. Rvachev,[3] A. Saha,[4] S. Širca,[3] R. Suleiman,[3] S. Strauch,[8] J. A. Templon,[12]
L. Todor,[18] P. E. Ulmer,[18] G. M. Urciuoli,[6] L. B. Weinstein,[18] K. Wijesooriya,[25]
B. Wojtsekhowski,[4] X. Zheng,[3] and L. Zhu[3]

(Jefferson Laboratory E91011 and Hall A Collaborations)

[1]*Department of Physics, University of Maryland, College Park, Maryland 20742, USA*
[2]*Florida State University, Tallahassee, Florida 32306, USA*
[3]*Massachusetts Institute of Technology, Cambridge, Massachusetts 02139, USA*
[4]*Thomas Jefferson National Accelerator Facility, Newport News, Virginia 23606, USA*
[5]*Saint Mary's University, Halifax, Nova Scotia, Canada B3H 3C3*
[6]*Istituto Nazionale di Fisica Nucleare, Sezione Sanità and Istituto Superiore di Sanità, Physics Laboratory, 00161 Roma, Italy*
[7]*California State University Los Angeles, Los Angeles, California 90032, USA*
[8]*Rutgers, The State University of New Jersey, Piscataway, New Jersey 08854, USA*
[9]*Florida International University, Miami, Florida 33199, USA*
[10]*University of Athens, Athens, Greece*
[11]*University of Regina, Regina, Saskatchewan, Canada S4S 0A2*
[12]*University of Georgia, Athens, Georgia 30602, USA*
[13]*CEA Saclay, F-91191 Gif-sur-Yvette, France*
[14]*University of New Hampshire, Durham, New Hampshire 03824, USA*
[15]*University of Lund, Box 118, SE-221 00 Lund, Sweden*
[16]*Université Blaise Pascal Clermont Ferrand et CNRS/IN2P3 LPC 63, 177 Aubière Cedex, France*
[17]*University of Massachusetts, Amherst, Massachusetts 01003, USA*
[18]*Old Dominion University, Norfolk, Virginia 23529, USA*
[19]*University of Virginia, Charlottesville, Virginia 22901, USA*
[20]*Renaissance Technologies Corporation, Setauket, New York 11733, USA*
[21]*Eastern Kentucky University, Richmond, Kentucky 40475, USA*
[22]*College of William and Mary, Williamsburg, Virginia 23187, USA*
[23]*Institut Jožef Stefan, University of Ljubljana, SI-1001 Ljubljana, Slovenia*
[24]*Norfolk State University, Norfolk, Virginia 23504, USA*
[25]*University of Illinois at Urbana-Champaign, Urbana, Illinois 61801, USA*

We measured angular distributions of recoil-polarization response functions for neutral pion electroproduction for $W = 1.23$ GeV at $Q^2 = 1.0$ (GeV/c)^2, obtaining 14 separated response functions plus 2 Rosenbluth combinations; of these, 12 have been observed for the first time. Dynamical models do not describe quantities governed by imaginary parts of interference products well, indicating the need for adjusting magnitudes and phases for nonresonant amplitudes. We performed a nearly model-independent multipole analysis and obtained values for Re $(S_{1+}/M_{1+}) = -(6.84 \pm 0.15)\%$ and Re $(E_{1+}/M_{1+}) = -(2.91 \pm 0.19)\%$ that are distinctly different from those from the traditional Legendre analysis based upon M_{1+} dominance and $\ell_\pi \leq 1$ truncation.

Insight into QCD-inspired models of hadron structure can be obtained by studying the properties of the nucleon and its low-lying excited states using electromagnetic reactions with modest spacelike four-momentum transfer, Q^2. In the very simplest models, quark-quark interactions with SU(6) spin-flavor symmetry suggest that the dominant configuration for the nucleon consists of three quarks in an S state with orbital and total angular momenta $L = 0$ and

$J = 1/2$, while the lowest excited state, the Δ resonance at $M_\Delta = 1.232$ GeV with $J = 3/2$, is reached by flipping the spin of a single quark and leaving $L = 0$. Thus, the pion electroproduction reaction for invariant mass $W \approx M_\Delta$ is dominated by the M_{1+} multipole amplitude. However, the $M_\Delta - M_N$ mass splitting and the nonzero neutron electric form factor clearly demonstrate that SU(6) symmetry is broken by color hyperfine interactions that introduce D-state admixtures with $L = 2$ into these wave functions [1]. Although quadrupole configurations cannot be observed directly in elastic electron scattering by the nucleon, their presence in both wave functions contributes to S_{1+} and E_{1+} multipole amplitudes for electroexcitation of the Δ. Additional contributions to these smaller multipoles may also arise from meson and gluon exchange currents between quarks [2] or coupling to the pion cloud outside the quark core [3,4]. Recently, it has also become possible to calculate N to Δ transition form factors using lattice QCD, albeit in the quenched approximation [5].

The relative strength of the quadrupole amplitudes is normally quoted in terms of the ratios SMR $=$ Re (S_{1+}/M_{1+}) and EMR $=$ Re (E_{1+}/M_{1+}) evaluated for isospin 3/2 at $W = M_\Delta$, but isospin analysis would require data for the $n\pi^+$ channel also. Fortunately, model calculations show that the isospin 1/2 contribution to these ratios is almost negligible. For example, one obtains (SMR, EMR) $= (-6.71\%, -1.62\%)$ for isospin 3/2 compared with $(-6.73\%, -1.65\%)$ for the $p\pi^0$ channel using MAID2003 [6] at $Q^2 = 1$ (GeV/c)^2 and $W = 1.23$ GeV. Therefore, we quote results for the $p\pi^0$ channel without making model-dependent corrections for the isospin 1/2 contamination.

Most previous measurements of the quadrupole amplitudes for Δ electroexcitation fit Legendre coefficients to angular distributions of the unpolarized cross section for pion production and employ a truncation that assumes: (1) only partial waves with $\ell_\pi \leq 1$ contribute and (2) terms not involving M_{1+} can be omitted. However, a more detailed analysis of multipole expansions for Legendre coefficients shows that neither assumption is sufficiently accurate [7]. The relative accuracy of such methods is no better than about 20%, but the statistical precision of modern experiments is potentially much better. Therefore, it is important to obtain data that are complete enough for nearly model-independent multipole analysis without relying upon sp truncation or M_{1+} dominance.

More detailed information about the nonresonant background can be obtained from polarization measurements that are sensitive to the relative phase between resonant and nonresonant amplitudes. This phase information is needed to test dynamical models that attempt to distinguish between the intrinsic properties of a resonance and the effects of rescattering. A few previous measurements of recoil polarization have been made for low Q^2 with the proton parallel to the momentum transfer [8,9], but their kine-

matic coverage is quite limited. Several recent measurements of beam analyzing power have also been made [10–12]. Those experiments demonstrated that recent dynamical models do not describe the nonresonant background well. More generally, there are 18 independent response functions for the $p(\vec{e}, e'\vec{p})\pi^0$ reaction, of which half are sensitive to real and half to imaginary parts of products of multipole amplitudes [13]. In this Letter we report angular distributions for 14 separated response functions plus 2 Rosenbluth combinations for $W = 1.23$ GeV at $Q^2 = 1.0$ (GeV/c)^2 that are sufficiently complete to perform a phenomenological multipole analysis; twelve of these response functions are obtained here for the first time. Data for a wider range of W will be presented later in a more detailed paper [14].

The observables for recoil polarization can be resolved into response functions according to

$$\bar{\sigma} = \nu_0[\nu_L R_L + \nu_T R_T + \nu_{LT} R_{LT} \sin\theta \cos\phi$$
$$+ \nu_{TT} R_{TT} \sin^2\theta \cos2\phi] \tag{1a}$$

$$A\bar{\sigma} = \nu_0[\nu'_{LT} R'_{LT} \sin\theta \sin\phi] \tag{1b}$$

$$P_n\bar{\sigma} = \nu_0[(\nu_L R_L^n + \nu_T R_T^n)\sin\theta + \nu_{LT} R_{LT}^n \cos\phi$$
$$+ \nu_{TT} R_{TT}^n \sin\theta \cos2\phi] \tag{1c}$$

$$P_\ell\bar{\sigma} = \nu_0[\nu_{LT} R_{LT}^\ell \sin\theta \sin\phi + \nu_{TT} R_{TT}^\ell \sin^2\theta \sin2\phi] \tag{1d}$$

$$P_t\bar{\sigma} = \nu_0[\nu_{LT} R_{LT}^t \sin\phi + \nu_{TT} R_{TT}^t \sin\theta \sin2\phi] \tag{1e}$$

$$P'_n\bar{\sigma} = \nu_0[\nu'_{LT} R'^n_{LT} \sin\phi] \tag{1f}$$

$$P'_\ell\bar{\sigma} = \nu_0[\nu'_{LT} R'^\ell_{LT} \sin\theta \cos\phi + \nu'_{TT} R'^\ell_{TT}] \tag{1g}$$

$$P'_t\bar{\sigma} = \nu_0[\nu'_{LT} R'^t_{LT} \cos\phi + \nu'_{TT} R'^t_{TT} \sin\theta], \tag{1h}$$

where $\bar{\sigma}$ is the virtual γN unpolarized cm cross section, A is the beam analyzing power, and P and P' are helicity-independent and helicity-dependent polarizations expressed in terms of longitudinal, normal, and transverse basis vectors $\hat{\ell} = \hat{p}_N$, $\hat{n} \propto \hat{q} \times \hat{\ell}$, and $\hat{t} \propto \hat{n} \times \hat{\ell}$. Here $\vec{q}$ is the momentum transfer in the lab and $\vec{p}_N$ is the final nucleon momentum in the πN cm frame. The response functions, R, depend upon W, Q^2, and $\cos\theta$, where θ is the pion angle relative to $\vec{q}$ in the cm frame; subscripts L and T represent longitudinal and transverse polarization states of the virtual photon while superscripts include the nucleon polarization component and/or a prime for beam polarization, as appropriate. Note that explicit factors of $\sin\theta$ have been removed so that the response functions reduce to polynomials in $\cos\theta$. It is also convenient to define the Rosenbluth combinations $\nu_T R_{L+T} = \nu_L R_L + \nu_T R_T$ and $\nu_T R_{L+T}^n = \nu_L R_L^n + \nu_T R_T^n$ for which separation would require variation of the beam energy, which was not performed in this experiment. The cm phase space is given by $\nu_0 = k/q_0$, where k and q_0 are the pion and equivalent real photon momenta, while the kinematical factors $\nu_T = 1$, $\nu_{TT} = \epsilon$, $\nu'_{TT} = \sqrt{1 - \epsilon^2}$, $\nu_L = \epsilon_S$, $\nu_{LT} = \sqrt{2\epsilon_S(1 + \epsilon)}$, $\nu'_{LT} = \sqrt{2\epsilon_S(1 - \epsilon)}$ are elements of the virtual photon density matrix based upon the transverse and scalar (lon-

gitudinal) polarizations, $\epsilon = (1 + 2\frac{\mathbf{q}^2}{Q^2}\tan^2\frac{\theta_e}{2})^{-1}$ and $\epsilon_S = \epsilon Q^2/\mathbf{q}^2$. Finally, ϕ is the angle between the scattering and reaction planes.

The experiment was performed in Hall A of Jefferson Laboratory using standard equipment described in Ref. [15]. A beam of 4531 ± 1 MeV electrons, with current ranging between about 40 and 110 μA, was rastered on a 15 cm LH$_2$ target. The beam polarization, averaging 72% for the first two running periods and 65% for the third, was measured nearly continuously using a Compton polarimeter, with systematic uncertainties estimated to be about 1% [16].

Scattered electrons and protons were detected in two high-resolution spectrometers, each equipped with a pair of vertical drift chambers for tracking and a pair of scintillation planes for triggering. Protons were selected using the correlation between velocity and energy deposition in plastic scintillators and pion production was defined by cuts on missing mass and the correlation between missing energy and missing momentum. The proton polarization was analyzed by a focal-plane polarimeter (FPP). Detailed descriptions of the FPP and its calibration procedures can be found in Refs. [17,18]. The electron spectrometer remained fixed at 14.1° with a central momentum of 3.66 GeV/c, while the proton spectrometer angle and momentum were adjusted to cover the angular distribution. Although the motion of the spectrometers was limited to the horizontal plane, the boost from cm to lab focuses the reaction into a cone with an opening angle of only 13° and provides enough out-of-plane acceptance to access all of the response functions, even those that vanish for coplanar kinematics. Cross sections were deduced by comparison with a Monte Carlo acceptance averaging of MAID2000 cross sections that includes radiative corrections and applies the experimental acceptance cuts for each setting. This model reproduces the observed distributions very well [19].

The nucleon polarization at the target in the cm frame was deduced from the azimuthal distribution for scattering in the FPP using the method of maximum likelihood. The likelihood function takes the form

$$\mathcal{L} = \prod_{\text{events}} \frac{1}{2\pi}(1 + \xi + \eta \cdot R), \qquad (2)$$

where ξ represents the false (instrumental) asymmetry, R is a vector containing the response functions, and η is a vector of eventwise calculable coefficients that depend upon kinematical variables, differential cross section, beam polarization and helicity, FPP scattering angles and analyzing power, and spin transport matrix elements. The system of equations derived from $\partial \ln\mathcal{L}/\partial R_m = 0$ is solved using an iterative procedure. The procedure was tested using pseudodata: a model was used to compute response functions for each accepted event, the predicted polarization was transported to the focal plane using the

same transport matrix as for the data analysis, and the azimuthal angle in the FPP was sampled according to its probability distribution. The pseudodata were then analyzed in the same manner as real data. We found that the model responses are recovered with fluctuations consistent with the statistical uncertainties. We also found that small deviations between acceptance-averaged and nominal Q^2 can be compensated using a dipole form factor.

Systematic uncertainties due to acceptance normalization, FPP analyzing power, beam polarization, elastic subtraction, false asymmetry, and spin rotation matrix elements were evaluated by comparing results from replays differing by a perturbation of the relevant parameter. The propagation of systematic uncertainties for fitted Legendre coefficients or multipole amplitudes was evaluated using fits to those data sets. Data for $W = 1.23$ GeV at $Q^2 = 1.0$ (GeV/c)^2 are shown in Fig. 1 for bin widths of $\Delta W = \pm 0.01$ GeV and $\Delta Q^2 = \pm 0.2$ (GeV/c)^2. We show R_{L+T}, R_{LT}, and R_{TT} extracted from the ϕ dependence of $\bar{\sigma}$ with error bars from fitting; the large error bars or missing bins for $\cos\theta \sim 0$ reflect inadequate ϕ coverage for this separation, but the phenomenological analyses use the actual differential cross sections. The bins of $\cos\theta$ for polarization were chosen to give approximately uniform statistics. Inner error bars with end caps show statistical uncertainties and outer error bars without end caps include systematic uncertainties. The systematic uncertainties in response functions and derived quantities are typically small compared with statistical or fitting uncertainties.

Figure 1 also shows predictions from several recent models: MAID2003 [6,20], DMT [21,22], SAID [23,24], and SL [25]. Although the first three response functions in column 1 and the last in column 3 have been observed before, the other 12 response functions have been observed here for the first time. The first two columns are determined by real parts of interference products and tend to be dominated by resonant amplitudes, while the last two columns are determined by imaginary parts that are more sensitive to nonresonant amplitudes. Thus, one finds relatively little variation among models for the first two columns and much larger variations for the last two, but none provides a uniformly good fit, especially to imaginary responses.

The response functions should be polynomials in $\cos\theta$ of relatively low order, especially if the assumption of M_{1+} dominance is valid near the Δ resonance. However, good fits over a range of W require additional terms in R_{LT}, R_{TT}, R'_{LT}, R^n_{L+T}, and R^ℓ_{TT}. The green dashed curves fit coefficients of Legendre expansions to the data for each response function independently, including terms beyond M_{1+} dominance as needed; the extra terms have negligible effect upon the SMR and EMR values obtained using the traditional truncation formulas. Our results for the Legendre analysis are compared with those of Joo *et al.* [26] for CLAS data in the top section of Table I. These Legendre results for EMR overlap, but our result for SMR
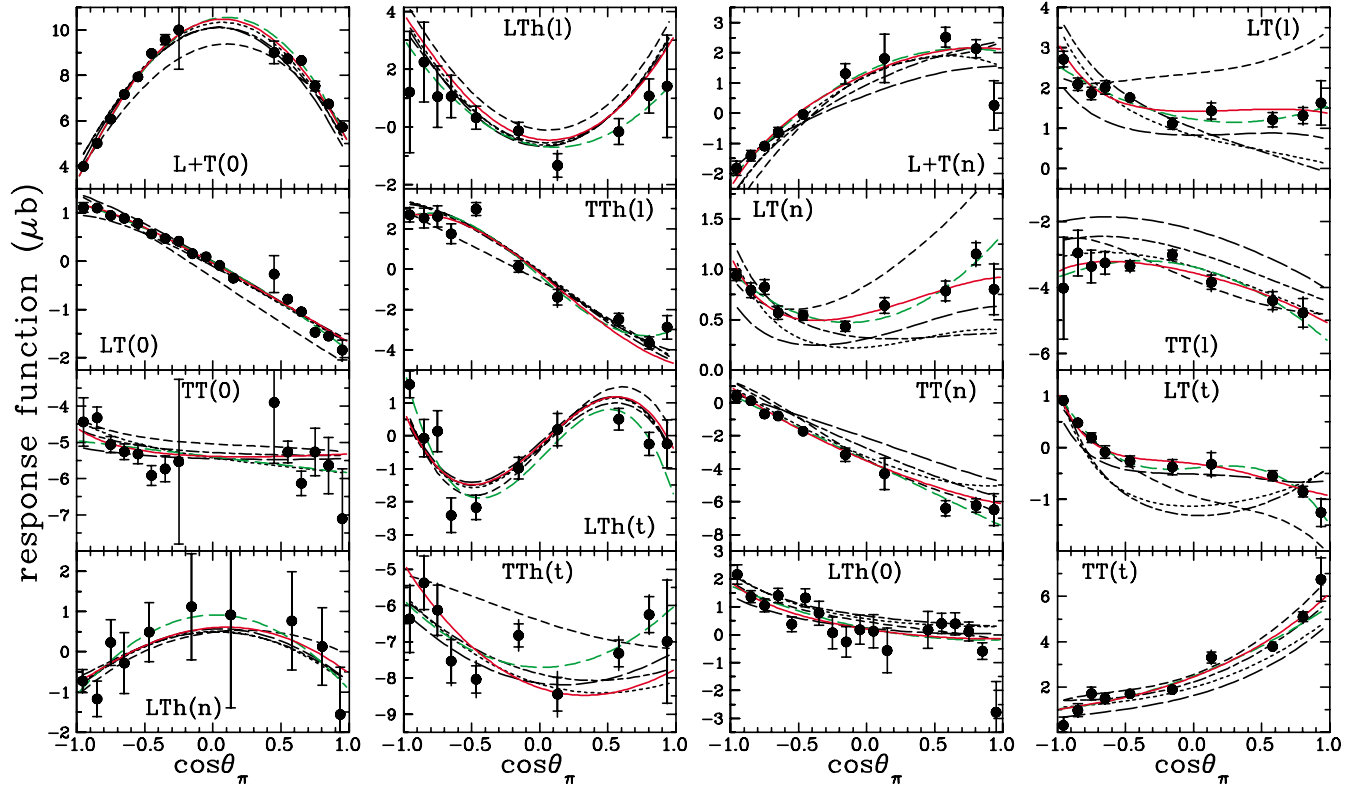
FIG. 1 (color online). Data for response functions at $W = 1.23$ GeV and $Q^2 = 1.0$ (GeV/$c)^2$ are compared with recent models and with fits. The labeling distinguishes L, T, LT, and TT contributions to the unpolarized (0) cross section and to transverse (t), normal (n), or longitudinal (l) components of recoil polarization with an h to indicate helicity dependence, if any. Linear combinations that cannot be resolved without Rosenbluth separation are identified by L + T. Black dash-dotted, dotted, short-dashed, and long-dashed curves represent the MAID2003, DMT, SAID, and SL models, respectively. The green mid-dashed curves show a Legendre fit while the solid red curves show a multipole fit.

is more precise and significantly smaller. Note that Joo *et al.* report typical (worst) truncation errors of 0.3(0.7)% for EMR and 0.1(0.5)% for SMR.

The solid red curves in Fig. 1 show a multipole analysis that varies the real and imaginary parts of all *s*-wave and *p*-wave amplitudes, except Im M_{1-}, plus real parts of $2-$ multipoles. Higher partial waves were determined using a baseline model, here based upon Born terms for pseudo-vector coupling. We did not vary Im M_{1-} because all models considered predict that it is negligible for our W range, yet experimentally it is strongly correlated with Im S_{1-}. Note that we could not achieve acceptable multipole fits without varying the *s*-wave amplitudes with respect to baseline models and we found that the imaginary part of S_{0+} is especially important. Fits starting from the MAID2003, DMT, or SL models are practically indistinguishable from those shown, but SAID is less suitable as a baseline model because some of its $\ell_\pi = 2$ amplitudes are too large. The insensitivity of quadrupole ratios to the choice of baseline model is shown in Table I. Therefore, the multipole analysis provides nearly model-independent quadrupole ratios; we choose as final the results based

upon the Born baseline to minimize residual theoretical bias.

Both Legendre and multipole analyses reproduce the data well but the multipole analysis is more fundamental, employs fewer parameters (16 versus 50), and uses the data for all response functions simultaneously while the more

TABLE I. Quadrupole ratios for $Q^2 = 1.0$ (GeV/$c)^2$. The first section reports Legendre analyses and the second multipole analyses based upon the specified baseline models.

Method/Baseline	SMR, %	EMR, %	χ^2_ν
Legendre	-6.11 ± 0.11	-1.92 ± 0.14	1.50
Joo *et al.*[a]	-7.4 ± 0.4	-1.8 ± 0.4	
Born	-6.84 ± 0.15	-2.91 ± 0.19	1.65
MAID2003	-6.90 ± 0.15	-2.79 ± 0.19	1.67
DMT	-6.82 ± 0.15	-2.70 ± 0.19	1.67
SL	-6.79 ± 0.15	-2.81 ± 0.19	1.64
SAID	-7.38 ± 0.15	-2.53 ± 0.20	1.85

[a]Weighted average of CLAS data for $Q^2 = 0.9$ (GeV/$c)^2$ from [26].
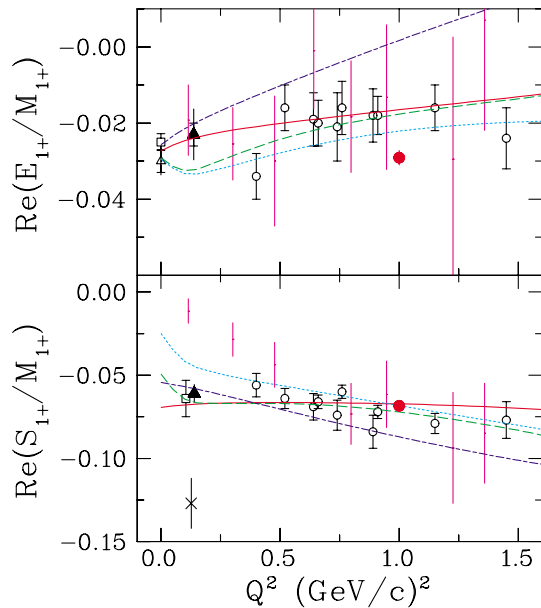
FIG. 2 (color online). Red circles, present results from multipole analysis; open squares, MAMI [9,27]; open triangles, LEGS [28]; filled triangles, MIT [29]; crosses, ELSA [30]; open circles, CLAS [26]. Small horizontal displacements are used to reduce clutter. Inner error bars with end caps show statistical and systematic errors; where available, outer error bars without end caps include model error. Red, green dashed, blue dash-dotted, and cyan dotted curves represent MAID2003, DMT, SAID, and SL, respectively. Magenta bars show lattice QCD results [5].

phenomenological Legendre analysis fits each response function independently and ignores the relationships between Legendre coefficients required by expansions of those coefficients in terms of products of multipole amplitudes. More detailed studies of those expansions [7,14] show that neither assumption of the traditional Legendre analysis is accurate and that truncation errors are particularly severe for EMR. Correct prediction of the number of appreciable Legendre coefficients does not ensure the accuracy of their multipole content. For example, using MAID2003 $p\pi^0$ multipoles, the contribution of Re $M_{1-}E_{1+}^*$ to the Legendre estimator for EMR is approximately -40% of the leading term for our kinematics. Nor are purely longitudinal contributions to the traditional EMR estimator negligible, yet Rosenbluth separation was not performed in Ref. [26] or in other recent experiments.

Recent data on quadrupole ratios for $Q^2 < 1.6 \, (\text{GeV}/c)^2$ are compared with representative models in Fig. 2. Note that the MAID2003, DMT, and SL models included previous EMR and SMR data in their parameter optimization. The present result for EMR disagrees strongly with the SAID prediction and is nearly identical to the data for $Q^2 = 0$, suggesting that EMR is nearly constant over this range. Unlike the somewhat smaller CLAS results for EMR, our multipole result does not depend upon sp truncation or M_{1+} dominance. Similarly, our SMR result is

close to those for $Q^2 < 0.2 \, (\text{GeV}/c)^2$, suggesting that SMR is nearly constant over this range also. The stronger Q^2 dependence of lattice QCD calculations [5] may arise because the quenched approximation misses pionic contributions that are expected to be important at low Q^2.

In summary, we have measured angular distributions of 14 separated response functions plus 2 Rosenbluth combinations for the $p(\vec{e}, e'\vec{p})\pi^0$ reaction at $Q^2 = 1.0 \, (\text{GeV}/c)^2$ across the Δ resonance, of which 12 have been obtained for the first time. Dynamical models describe responses governed by real parts of interference products relatively well, but differ both from each other and from the data more strongly for imaginary parts that are more sensitive to nonresonant mechanisms. None of the theoretical models considered provides a uniformly good description of the polarization data. We performed a nearly model-independent multipole analysis and obtained SMR $= -(6.84 \pm 0.15)\%$ and EMR $= -(2.91 \pm 0.19)\%$. The traditional Legendre analysis also fits the data well but gives distinctly smaller quadrupole ratios, demonstrating that its assumptions about the relative magnitudes and phases of multipoles are not sufficiently accurate. A more detailed presentation of the fitted multipole amplitudes will be given in a longer paper.

[1] N. Isgur, G. Karl, and R. Koniuk, Phys. Rev. D **25**, 2394 (1982).
[2] A. J. Buchmann and E. M. Henley, Phys. Rev. C **63**, 015202 (2001).
[3] M. Fiolhais, G. Golli, and S. Sirca, Phys. Lett. B **373**, 229 (1996).
[4] S. S. Kamalov and S. N. Yang, Phys. Rev. Lett. **83**, 4494 (1999).
[5] C. Alexandrou *et al.*, Phys. Rev. Lett. **94**, 021601 (2005).
[6] D. Drechsel *et al.*, A Unitary Isobar Model for Pion Photo and Electroproduction on the Nucleon, www.kph.uni-mainz.de/maid/maid2003.
[7] J. J. Kelly, nucl-ex/0507010 [Phys. Rev. C (to be published)].
[8] G. A. Warren *et al.*, Phys. Rev. C **58**, 3722 (1998).
[9] T. Pospischil *et al.*, Eur. Phys. J. A **12**, 125 (2001).
[10] P. Bartsch *et al.*, Phys. Rev. Lett. **88**, 142001 (2002).
[11] K. Joo *et al.*, Phys. Rev. C **68**, 032201 (2003).
[12] C. Kunz *et al.*, Phys. Lett. B **564**, 21 (2003).
[13] A. S. Raskin and T. W. Donnelly, Ann. Phys. (N.Y.) **191**, 78 (1989).
[14] J. J. Kelly *et al.* (unpublished).
[15] J. Alcorn *et al.*, Nucl. Instrum. Methods Phys. Res., Sect. A **522**, 294 (2004).

[16] S. Escoffier, Ph.D. thesis, University of Paris, 2001.

[17] R. E. Roché, Ph.D. thesis, Florida State University, 2003.

[18] V. Punjabi *et al.*, Phys. Rev. C **71**, 055202 (2005).

[19] Z. Chai, Ph.D. thesis, Massachusetts Institute of Technology, 2003.

[20] D. Drechsel *et al.*, Nucl. Phys. **A645**, 145 (1999).

[21] S. S. Kamalov *et al.*, Phys. Rev. C **64**, 032201(R) (2001).

[22] D. Drechsel *et al.*, A Dynamical Model for Pion Photo and Electroproduction on the Nucleon, www.kph.uni-mainz. de/maid/dmt.

[23] R. A. Arndt *et al.*, in *Proceedings of the Workshop on the Physics of Excited Nucleons (NSTAR2002)*, edited by S. A. Dytman and E. S. Swanson (World Scientific, Singapore, 2003).

[24] R. A. Arndt *et al.*, gwdac.phys.gwu.edu.

[25] T. Sato and T.-S. H. Lee, Phys. Rev. C **63**, 055201 (2001).

[26] K. Joo *et al.*, Phys. Rev. Lett. **88**, 122001 (2002).

[27] R. Beck *et al.*, Phys. Rev. C **61**, 035204 (2000).

[28] G. Blanpied *et al.*, Phys. Rev. Lett. **79**, 4337 (1997).

[29] N. F. Sparveris *et al.*, Phys. Rev. Lett. **94**, 022003 (2005).

[30] F. Kalleicher *et al.*, Z. Phys. A **359**, 201 (1997).